# Empirical and numerical study of wind loading on a high-rise building

Bodhinanda Chandra[1], Mayu Sakuma[2], Rishith Ellath Meethal[1]

## Abstract

*Wind loading are a crucial consideration in the design of various civil engineering structures, such as high-rise buildings, wind turbines, or bridges, since the accurate understanding and prediction of impact loads by wind can provide an important information on structural safety assessment. Such study is extremely beneficial to analyze the vibration effect of tall buildings under the influence of wind flow, which by further may lead to the improvement of structural design to satisfy the safety, comfort and performance criteria. Coming with this motivation, two different approaches, i.e. empirical studies of the building design codes and numerical simulations, are performed on the Empire State Building in Manhattan, New York, which we took as an example for our study. First, the effect of wind on a simplified model of the building is analyzed by referring to a design specification and regulations published by the American Society of Civil Engineering (ASCE). Furthermore, a CFD simulation considering simplified building model in an air-flow is implemented within the OpenFoam framework. We also conducted a simple structural analysis using a simple multi-degree of freedom (MDOF) systems without damping to estimate the structural modes and eigen-frequencies. In order to validate our works, a comparison test is also done in a two-dimensional FSI simulation implemented in Kratos Multiphysics considering the two-way strong coupling FSI scheme on a particular building cross section. A good agreement between the numerical results demonstrates the success of the implemented approach.*

**Keywords:**

wind-induced vibration, structural design and analysis, computational fluid dynamics, fluid-structure interaction

## 1 Introduction

Wind engineering is a crucial part of many construction projects, particularly high-rise buildings. At heights of 400m and above, the measured wind flow is, at some degree, similar to that experienced by an airplane. The effect of wind is, therefore, a very important issue, at the same time challenging, in the building and structural engineering field. It is said that almost 70-80% of economic losses due to natural disasters in the world are caused by extreme winds and related water hazards [13]. The risk of future disasters continues to escalate with population shifts towards urban, and thus, further assessment and consideration on this "Multi-physics" phenomena is important.

The term "Multi-physics" stands for a engineering discipline that studies multiple interacting physical phenomena in computer simulations. For instance, the fluid-structure interaction (FSI) is a study of mutual influence between a fluid in rest or in flow and a flexible or moving structure. In order to understand such complicated phenomena, analytical solutions to the model equations are impossible to obtain, whereas laboratory experiments are limited in scope and scale; thus in order to investigate the fundamental physics involved in the interaction, numerical simulations may be employed. Methods to

1 Graduate Student, Computational Mechanics Program, Department of Civil, Geo, and Environmental Engineering, Technical University of Munich
2 PhD Student, Chair of Structural Analysis, Department of Civil, Geo, and Environmental Engineering, Technical University of Munich

efficiently and accurately model the behavior of these complex systems are indeed in great economic and environmental demands. In the context of the structural wind engineering of high-rise buildings, FSI approach is generally used to predict the flow-induced vibration and estimate the forces exerted by the surrounding wind flow as it sometimes can be considerably large. However, FSI simulations are not always easy and feasible to conduct due to its considerably complicated algorithm and communication scheme which sometime requires high computational resources. The aim of this project is to represent the Multi-physics study of wind-structure interaction in a simpler manner. This project will mainly focus on the implementation of a wind flow simulation, in a relatively simple yet comprehensive fashion, followed by the assessment of design criteria of high-rise structures from the structural engineering and design perspective.


Figure 1: Empire State Building in New York [8]

The aforementioned analyses are performed for the Empire State Building, which is a 102-story tall (380m) skyscraper located in Midtown Manhattan, New York. The geometrical and mechanical dimensions of the building are only approximated omitting minor details, whereas for the geometrical location, the terrain category and the wind intensity are truly adapted according to the available data [2]. The geometric and material parameters of the buildings are considered as follow:

| Level | $H$[m] | $K$[N/m] | $A$[m$^2$] | $M$[ton] |
|---|---|---|---|---|
| $0 \sim 6$ | $0.0 \sim 22.4$ | $1.24 \times 10^{15}$ | 4724.72 | 8073 |
| $7 \sim 20$ | $22.4 \sim 76.25$ | $6.4 \times 10^{14}$ | 3583.58 | 6156 |
| $21 \sim 30$ | $76.25 \sim 110.55$ | $5.62 \times 10^{14}$ | 2928.44 | 4363 |
| $31 \sim 80$ | $110.55 \sim 290.30$ | $3.24 \times 10^{14}$ | 2319.03 | 3657 |
| $81 \sim 102$ | $290.30 \sim 380.00$ | $2.0 \times 10^{12}$ | 100.00 | 122 |

Table 1: Geometry and material characteristics of Empire State Building

where, $H$, $K$, $A$, and $M$, are the approximated height, assumed stiffness, floor area, and mass of the building respectively. As there are no technical data available for the mass and stiffness, some simplifications and assumptions are used to find the above values. In order to distribute the total mass to different floor

sections, the building is divided into six parts according to different cross section area. Then, the whole mass of the building is distributed to each part considering it's volume fraction; we assume the specific density of materials in all sections are the same. The section masses are further distributed to each floor uniformly. Moreover, the stiffness of each floor can be approximated by assuming it as a 1D cantilever beam with a hollow rectangular cross section. Here, the standard formula $K = \frac{12EI}{L^3}$ is assumed.

In the current project, a computational wind engineering (CWE) simulation is implemented in an open source computational fluid dynamics (CFD) software, the OpenFoam, to estimate the wind loading exerted on the building. The recorded wind loading is then compared with a hand-calculated value which can be computed taken into account the wind profile and velocity given by the American Society of Civil Engineering (ASCE). Furthermore, the frequency of the recorded wind forces is also compared with the dominant eigen-frequencies of the building which can be estimated from a simple 1D MDOF structure simulation. Last but not least, a simple 2D FSI simulation is conducted in Kratos Multi-physics in order to validate the forces and the wind-induce vibration caused by the vortex shedding. Thus, the content of the project is structured in four sections: The second chapter introduces the theoretical background for all components of the simplified FSI calculation and simulation. Fluid solvers, structural solvers, and corresponding coupling mechanisms are introduced and discussed separately in addition to the wind profile modeling adapted from the ASCE. Section three is dedicated to the results and validation of our simulations and calculation. This includes a cross-check of the hand-calculated ASCE method for forces and moments, CFD simulations performed in OpenFoam, functionality of the simplified structural model and a plausibility study and validation of our 2D FSI simulation. Finally, the last chapter contains a summary of the project work and offers an outlook at possible future extensions.

# 2 Underlying Theory

## 2.1 Wind Flow Modeling in CFD Simulations

### 2.1.1 Governing Equations

The governing equations of the fluid flow, the continuity and the Navier-Stokes equation for incompressible Newtonian fluids, are represented as,

$$\nabla \cdot \boldsymbol{v} = 0 \tag{1}$$

$$\frac{D\boldsymbol{v}}{Dt} = \frac{\partial \boldsymbol{v}}{\partial t} + (\boldsymbol{v} \cdot \nabla)\boldsymbol{v} = -\frac{1}{\rho_0}\nabla P + \nu \nabla^2 \boldsymbol{v} + \boldsymbol{g} \tag{2}$$

where $\boldsymbol{v}$ is the velocity field, $P$ is the pressure, $\rho$ is the density, and $\nu$ is the molecular kinematic viscosity of the fluid, respectively. Here, $\boldsymbol{g}$ and $t$ indicate the gravitational acceleration and time. In the most general incompressible flow approach, the density is assumed to be constant, with its initial value $\rho_0$.

### 2.1.2 Inlet Velocity Profile

In order to model our inlet wind profile as accurate as possible, we have referred to the measurement of wind speed data given by ASCE [2] as illustrated in Figure 2. According to the ASCE design regulation, we assumed that the basic wind speed in Mid-Manhattan area is $V = 104$mph or about $V = 46.5$m/s. We

can then determine the velocity pressure $q_z$ for wind speed $V$ by the following equation:

$$\begin{aligned} &(\text{In Imperial units}) && q_z = 0.00256 K_z K_{zt} K_d V^2 I[\text{lbf/ft}^2] \\ &(\text{In SI units}) && q_z = 0.0613 K_z K_{zt} K_d V^2 I[\text{N/m}^2] \end{aligned} \tag{3}$$

where, $K_z, K_{zt}$, and $K_d$ are the velocity pressure exposure coefficient, topographic factor, and wind directionality factor, respectively. Here, the importance factor $I$ is used to adjust the level of structural reliability of a building to be consistent with the building classification.

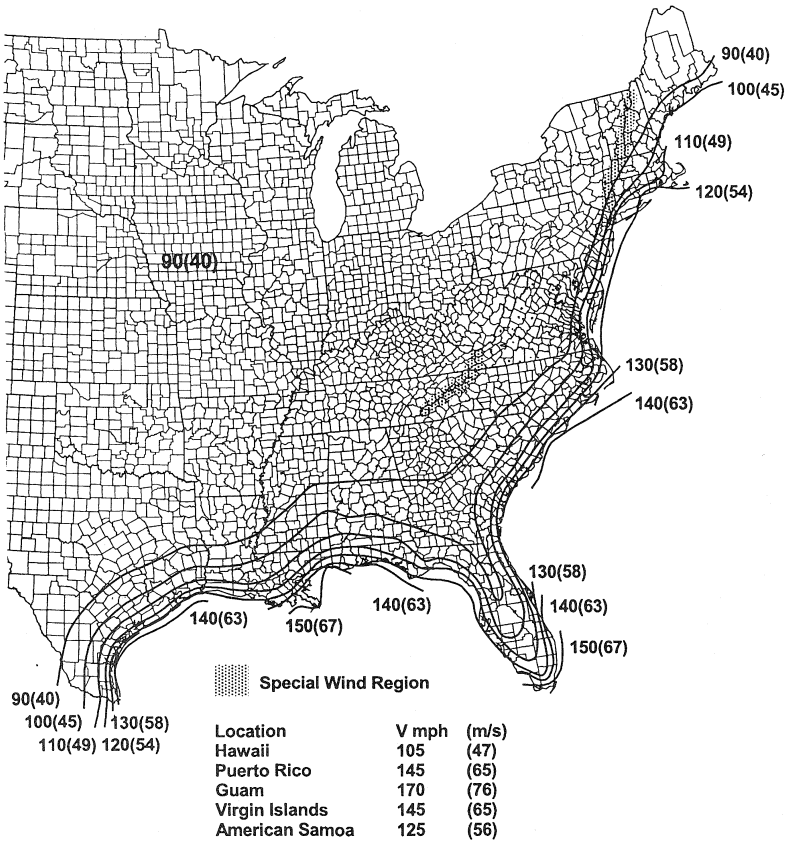


Figure 2: Basic wind speed data at the east coast of the USA [2]

Since all the parameter specified in the design codes are assumed in imperial units, all the calculated value here is first assumed in the same unit system and, at the end of the calculation, the conversion from imperial units to SI will be performed. The velocity pressure exposure coefficient can be calculated by the following equation, which is a function of height $z$[ft], while the remaining factors are given in the following table with calculation specified in details within the ASCE design codes.

$$K_z(z) = 2.01(z/z_g)^{\frac{2}{\alpha}} \tag{4}$$

| $Z_g$[ft] | $\alpha$ | $K_d$ | $K_{zt}$ | $I$ |
|---|---|---|---|---|
| 1200 | 7 | 0.85 | 1.0 | 1.15 |

Table 2: Necessary parameters for velocity pressure calculation referred from [2]

Following this, we can also obtain the velocity profile at changing height $U(z)$ as:

$$q_z = \frac{1}{2}\rho_{\text{air}}U^2 \tag{5}$$

$$U(z) = \sqrt{2q_z/\rho_{\text{air}}} \tag{6}$$

### 2.1.3 Turbulence Modeling

When dealing with the turbulent flows, the turbulent stress term which can be derived from the nonlinear convective term in (2) needs to be modeled. In our CFD simulation, two methods are used to model the energy dissipation caused by turbulence; the Reynolds Averaging Navier Stokes (RANS) and the Large Eddy Simulation (LES) which will be explained thoroughly in the following sections.

#### Reynolds Averaged Navier Stokes (RANS) Model

The Reynolds-averaged NavierâĂŞStokes equations (or RANS equations) are time-averaged equations of motion for fluid flow. The idea behind the equations is nothing but the Reynolds decomposition, whereby an instantaneous quantity $\phi(\boldsymbol{x},t)$ is decomposed into its time-averaged $\phi)\bar{(}\boldsymbol{x})$ and fluctuating quantities $\phi'(\boldsymbol{x},t)$, an idea first proposed by Osborne Reynolds. The RANS equations are primarily used to describe turbulent flows and can be written as the following equation after averaging (2):

$$\frac{\partial}{\partial t}(\rho_0\overline{\boldsymbol{v}}) + \nabla\cdot(\rho_0\overline{\boldsymbol{v}}\otimes\overline{\boldsymbol{v}}) = \boldsymbol{g} - \nabla(\overline{p} + \frac{2}{3}\rho_0 k) + \nabla\cdot(\mu\nabla\overline{\boldsymbol{v}}) + \nabla\cdot\left[\mu\mathbf{dev2}\left((\nabla\overline{\boldsymbol{v}})^T\right)\right] - \nabla\cdot[\rho_0\boldsymbol{R}_{\text{dev}}] \tag{7}$$

where,

$$\boldsymbol{R}_{\text{dev}} = \overline{\boldsymbol{v}'\otimes\boldsymbol{v}'} - \frac{2}{3}k\boldsymbol{I} \tag{8}$$

The objective of the turbulence models for the RANS equations is to model the Reynolds stresses $\rho_0\overline{v'\otimes v'}$, which can be done by three main categories of RANS-based turbulence models: 1) Linear eddy viscosity models, 2) Nonlinear eddy viscosity models, or 3) Reynolds stress model (RSM). In the current project, the $k-\epsilon$ model, which is a two equation model considering turbulence kinetic energy, $k$, and turbulence dissipation rate, $\epsilon$, is used in OpenFoam to model the turbulence. Here, the turbulence kinetic energy equation is given by:

$$\frac{D}{Dt}(\rho_0 k) = \nabla\cdot(\rho_0 D_k\nabla k) + G_k - \frac{2}{3}\rho_0\left(\nabla\cdot\boldsymbol{v}\right)k - \rho_0\epsilon + S_k \tag{9}$$

and the dissipation rate by:

$$\frac{D}{Dt}(\rho_0\epsilon) = \nabla\cdot(\rho_0 D_\epsilon\nabla\epsilon) + \frac{C_1 G_k\epsilon}{k} - \left(\frac{2}{3}C_1 + C_{3,RDT}\right)\rho_0\left(\nabla\cdot\boldsymbol{v}\right)k - C_2\rho_0\frac{\epsilon^2}{k} + S_\epsilon \tag{10}$$

Here, all the default model coefficients which can be found in details at [5] are used.

#### Large Eddy Simulation (LES) Model

The principal idea behind LES is to reduce the computational cost by ignoring the smallest length scales, which are the most computationally expensive to resolve, via low-pass filtering of the Navier-Stokes equations. Such a low-pass filtering, which can be viewed as a time- and spatial-averaging, effectively removes small-scale information from the numerical solution. This information is not irrelevant, however, and its effect on the flow field must be modeled. Mathematically, one may think of separating the velocity field into a resolved and sub-grid part. The resolved part of the field represent the "large" eddies, while

the sub-grid part of the velocity represent the "small scales" whose effect on the resolved field is included through the sub-grid-scale model. Formally, one may think of filtering as the convolution of a function with a filtering kernel G.

In our CFD simulation, the k Equation LES model is assumed. Here, the turbulence kinetic energy equation is given by:

$$\frac{D}{Dt}\rho_0 k = \nabla \cdot (\rho_0 D_k \nabla k) + \rho_0 G - \frac{2}{3}\rho_0 k \nabla \cdot \boldsymbol{v} - \frac{C_e \rho_0 k^{1.5}}{\Delta} + S_k \tag{11}$$

along with the following filtered Navier-Stokes equation:

$$\frac{\partial \overline{\boldsymbol{v}}}{\partial t} + \nabla \cdot (\overline{\boldsymbol{v}} \otimes \overline{\boldsymbol{v}}) = \boldsymbol{g} - \frac{1}{\rho_0}\nabla \overline{p} + 2\nu \nabla \cdot \boldsymbol{S} - \nabla \cdot \boldsymbol{\tau}^r \tag{12}$$

Here, all the default model coefficients which can be found in details at [6] are used.

### 2.1.4 Numerical Methods

**Finite Volume Method in OpenFOAM**

The fluid domain in our CFD simulation and its governing equation are discretized in Finite Volume approach and the simulation is conducted in OpenFOAM [7], a widely used open-source Computational Fluid Dynamics (CFD) software which is based on C++ frameworks. The popularity of the Finite Volume Method (FVM) in CFD stems from the high flexibility it offers as a numerical method, where the discretization is carried out directly in the physical space without the necessity of transformation of physical and computational coordinate system. Moreover, its adoption of a collocated arrangement [12] made it suitable for solving flows in complex geometries. These developments have expanded the applicability of the FVM to encompass a wide range of fluid flow simulations in various applications while retaining the simplicity of its mathematical formulation.

In the FVM manner, the conservation equation (1) and (2) should be writen in its weak or integral form as,

$$\int_\Gamma \boldsymbol{v} \cdot \boldsymbol{n} d\Gamma = 0 \tag{13}$$

$$\underbrace{\frac{\partial}{\partial t}\left(\rho \int_\Omega \boldsymbol{v} d\Omega\right)}_{\text{transient term}} + \underbrace{\rho \int_\Gamma \boldsymbol{v}(\boldsymbol{v} \cdot \boldsymbol{n}) d\Gamma}_{\text{convective term}} = \underbrace{-\int_\Gamma P \boldsymbol{n} d\Gamma}_{\text{pressure term}} + \underbrace{\int_\Gamma \mu(\nabla \boldsymbol{v}) \cdot \boldsymbol{n} d\Gamma}_{\text{diffusive term}} + \underbrace{\rho \boldsymbol{g} \Omega}_{\text{source term}} \tag{14}$$

Here, $\int_\Omega$ and $\int_\Gamma$ are the volume and surface integrals over volume $\Omega$ and surface $\Gamma$, respectively. Notice that the transformation of integral form from volume integral and surface integral and vice versa can be performed through the use of the Gauss theorem. The following procedure necessary is then to approximate these volumes and faces integrals in each discrete element which can be evaluated in various approach taking into account the order of accuracy, boundary conditions, integration schemes, and, most importantly, computational FVM mesh (whether structured or unstructured, or whether staggered or collocated). Several possible approximations and interpolation methods and its implementation in OpenFOAM are clearly explained and described in [10].

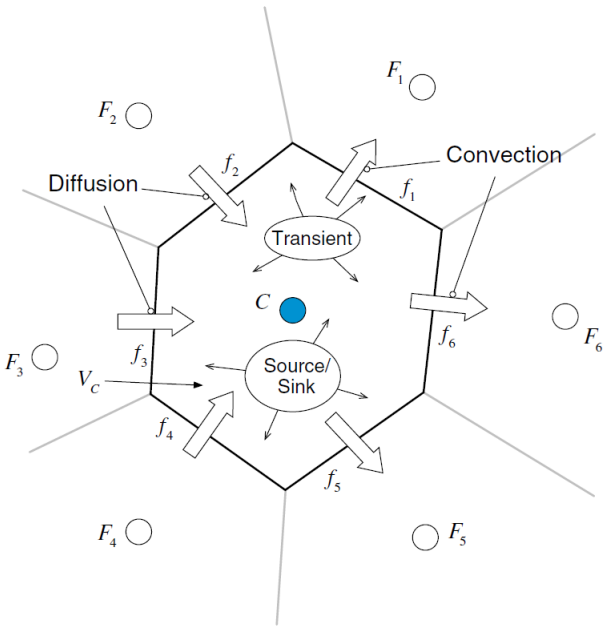


Figure 3: Conservation in a discrete Finite Volume element [10]

**Finite Element Method in Kratos Multiphysics**

For the fluid solver in our FSI simulation performed in Kratos, the weak formulation of the Navier Stokes Equation in the standard Galerkin finite element formulation is used. This requires a local approximation for the velocity ($\boldsymbol{v} \approx \boldsymbol{v}^h$) and for the pressure ($p \approx p^h$) by means of shape functions. Besides this (finite dimensional) solution function space, a second space for the test functions has to be defined. Both contain functions of the Sobolev space $\mathcal{H}^1(\Omega)$ with $\Omega$ representing the computational domain. The following affiliations can be noted:

- $\boldsymbol{v} \in \mathcal{H}^1_D = \{v \in \mathcal{H}^1(\Omega) \mid v \in \mathcal{P}_m \; and \; v = v_D \; on \; \Gamma_{Dirichlet}\}$ states, that the velocity solution has to fulfill the Dirichlet boundary conditions.
- $\boldsymbol{w} \in \mathcal{H}^1_0 = \{w \in \mathcal{H}^1(\Omega) \mid w \in \mathcal{P}_m \; and \; w = 0 \; on \; \Gamma_{Dirichlet}\}$ sets the makes the velocity test functions vanish on a Dirichlet boundary.
- $p, q \in \mathcal{L}^2(\Omega)$ states that both the pressure and its test function must be square-integrable functions.

Under these definitions, the Galerkin weak form of the NSE can now be stated using the abbreviating notations $(a,b) = \int_\Omega a \cdot b \, d\Omega$:

$$\begin{aligned} \rho \left(\frac{\partial \boldsymbol{v}}{\partial t}, \boldsymbol{w}\right) + \rho(\boldsymbol{v} \cdot \nabla)\, \boldsymbol{v} - \mu \left(\nabla \boldsymbol{v}, \nabla \boldsymbol{w}\right) + (p, \nabla \boldsymbol{w}) &= \rho \left(\boldsymbol{f}, \boldsymbol{w}\right) + (\boldsymbol{w}, \boldsymbol{t})_{\Gamma_N} \\ (q, \nabla \cdot \boldsymbol{v}) &= 0 \end{aligned} \tag{15}$$

After the introduction of the spatial discretization, the resulting spatial finite element discretization of the weak form can be written in a matrix form. The convection matrix $\boldsymbol{C}$ and the load vector $\boldsymbol{F}$ depend on the unknown $\boldsymbol{v}$, which introduces non-linearity:

$$\boldsymbol{M}\,\frac{\partial \boldsymbol{v}(t)}{\partial t} + [\boldsymbol{C}(\boldsymbol{v}(t)) + \mu\,\boldsymbol{L}]\,\boldsymbol{v}(t) + \boldsymbol{G}\,p(t) = \boldsymbol{F}(\boldsymbol{v}(t))$$
$$\boldsymbol{G}^T\,\boldsymbol{v}(t) = 0 \tag{16}$$

The involved matrices are calculated as follows:
Mass matrix

$$\boldsymbol{M} = \rho \int_\Omega \boldsymbol{N}\,\boldsymbol{N}^T\,d\Omega \tag{17}$$

Laplacian matrix

$$\boldsymbol{L} = \int_\Omega \nabla\boldsymbol{N}\,\nabla\boldsymbol{N}^T\,d\Omega \tag{18}$$

Gradient matrix

$$\boldsymbol{G} = -\int_\Omega \nabla\boldsymbol{N}\,\boldsymbol{N}\,d\Omega \tag{19}$$

Convection matrix

$$\boldsymbol{C}(\boldsymbol{v}) = \rho \int_\Omega \boldsymbol{N}\,(\boldsymbol{v}\,\nabla\boldsymbol{N})\,d\Omega \tag{20}$$

Load vector

$$\boldsymbol{F}(\boldsymbol{v}) = \int_\Omega \boldsymbol{N}\boldsymbol{f}\,d\Omega + \int_{\Gamma_N} \boldsymbol{n}\cdot(p\boldsymbol{I} - \mu\nabla\boldsymbol{v})\,d\Gamma \tag{21}$$

In addition, a time integration scheme is necessary to complete the solution of the problem. Ideally it should be chosen such that it is both stable and accurate. Without taking special care when choosing an element type, an immediate numerical solution of the presented Galerkin finite element formulation can fail because spurious oscillations occur. As a consequence, stabilization techniques, such as the Variational Multi Scale (VMS), must be applied.

## 2.2 Structural Analysis and Design

Analyzing the Empire State Building in a full model is numerically expensive. Therefore, in the current project, we model the building as a simple one-dimensional multi-degree of freedoms (1D MDOF) system with spring in between the mass elements. The section below explains the basics related to MDOF system and its implementation for the analysis of Empire State Building.

### 2.2.1 Multiple Degree of Freedom Systems

In general, a dynamic system can be analyzed via the balance of internal and external forces acting on it. When it is reduced to an SDOF system, all the relevant effects can be attributed to one of three main components: a conservative stiffness value $k$, a non-conservative dissipation (or dampening) coefficient $c$, and the inertial response due to the mass $m$. So, for a design variable $u$, the equation is

$$m\ddot{u}(t) + c\dot{u}(t) + ku(t) = F(t) \tag{22}$$

where $F(t)$ represents the external force acting on the structure.
In a MDOF system the interaction between each DOF are also considered. This results in similar equation as above but with mass, stiffness and damping matrix instead of the single values. For instance, for the

basic 2 DOF freedom system, the equation takes the form as:

$$\begin{bmatrix} m_1 & 0 \\ 0 & m_2 \end{bmatrix} \begin{Bmatrix} \ddot{u}_1 \\ \ddot{u}_2 \end{Bmatrix} + \begin{bmatrix} c_1 + c_2 & -c_2 \\ -c_2 & c_2 \end{bmatrix} \begin{Bmatrix} \dot{u}_1 \\ \dot{u}_2 \end{Bmatrix} + \begin{bmatrix} k_1 + k_2 & -k_2 \\ -k_2 & k_2 \end{bmatrix} \begin{Bmatrix} u_1 \\ u_2 \end{Bmatrix} = \begin{Bmatrix} F_1 \\ F_2 \end{Bmatrix} \tag{23}$$

For the specific case of Empire state building, each floor is considered as a DOF, and thus, we have total 102 DOFs. The equation is solved using a simple python code to obtain two kinds of solutions; one is the first three eigen-frequencies and modes of oscillation and second the displacement due to applied wind load. Here, we omit the dampening effect since accurate data of damping constant in the building is not available. As we modeled the structure into a 1D cantilever beam, the mass and stiffness results in a diagonal lumped mass matrix and a tridiagonal stiffness matrix written as:

$$K = \begin{bmatrix} 2k & -k & 0 & \cdots & 0 \\ -k & 2k & -k & \cdots & \vdots \\ 0 & \ddots & \ddots & \ddots & 0 \\ \vdots & & \ddots & 2k & -k \\ 0 & \cdots & \cdots & -k & k \end{bmatrix} \tag{24}$$

The static wind load $\boldsymbol{F}$ here was taken from the velocity profile generated using the available design code.

### 2.2.2 The Generalized-$\alpha$ integration method

One of the key elements that a numerical scheme should provide in solving linear (and non-linear) dynamic problems, comes in the form of numerical dissipation for higher frequencies due to the choice of space and/or time discretization. Some popular schemes which satisfy this are the implicit one step methods such as the Newmark-$\beta$ and the Hilber-Hughes-Taylor (HHT-$\alpha$), which offer second order accuracy for linear dynamic problems and are suitable for varying time step sizes. The Generalized-$\alpha$ method takes from these methods and refers to a more general class of methods, thus extending the applicability of these strategies to a broader range of problems. Specifically, by means of varying $\rho_\infty$, the spectral radius at infinity, the amount of numerical dissipation of the method can be tuned.

In this scheme, the integration is performed with an auxiliary point defined via two parameters $\alpha_M$ and $\alpha_F$ (hence the name of the method) which depend on $\rho_\infty$, such that the balance equation becomes:

$$m \cdot \ddot{u}_{t+\alpha_M \Delta t} + c \cdot \dot{u}_{t+\alpha_F \Delta t} + k \cdot u_{t+\alpha_F \Delta t} = F_{t+\alpha_F \Delta t} \tag{25}$$

with the definitions:

$$\begin{aligned} u_{t+\alpha_F \Delta t} &= (1-\alpha_F) u_t + \alpha_F u_{t+\Delta t} \\ \dot{u}_{t+\alpha_F \Delta t} &= (1-\alpha_F) \dot{u}_t + \alpha_F \dot{u}_{t+\Delta t} \\ \ddot{u}_{t+\alpha_M \Delta t} &= (1-\alpha_M) \ddot{u}_t + \alpha_M \ddot{u}_{t+\Delta t} \end{aligned} \tag{26}$$

The values at the end of the step, in turn, are calculated by the Newmark approximations:

$$u_{t+\Delta t} = u_t + \Delta t \dot{u}_t + \Delta t^2 \left( \left( \frac{1}{2} - \beta \right) \ddot{u}_t + \beta \ddot{u}_{t+\Delta t} \right) \tag{27}$$

$$\dot{u}_{t+\Delta t} = \dot{u}_t + \Delta t \left( (1-\gamma) \ddot{u}_t + \gamma \ddot{u}_{t+\Delta t} \right) \tag{28}$$

The system is thus solved implicitly for a given initial displacement and velocity, by combining (25), (26), (27), and (28) with the initial acceleration approximated as:

$$\ddot{u}_0 = m^{-1}(F_0 - c \cdot \dot{u}_0 - k \cdot u_0) \tag{29}$$

Further information on this method and its properties can be found in [3] and in [1].

## 2.3 Fluid-Structure Interaction (FSI)

The basic idea of an FSI scheme in CWE is to connect the mechanical behavior between two completely different systems, the structure and the wind, which have different mathematical models and physical behavior. In addition to that, the FSI scheme also acts as an interface between them, which generally provides a way to connect the two distinct solvers or rules the flow of information from one system to another. In our 2D FSI simulation, the *staggered* or *partitioned* approach is assumed. Here, we keep the fluid and the structure solvers separated as two distinct blocks of solver which has been implemented nicely for 2D SDOF system in Kratos. We also employ the *strongly two-way coupling* approach where the convergence at the boundary between structure and fluid is considered.

### 2.3.1 FSI Coupling Scheme

In our validation test, the 2D staggered two-way strongly coupled FSI scheme is chosen. The FSI interface is implemented to firstly transfer the fluid pressure force acting at the structure to the structure solver. The force transferred will further cause deformation on the structure and this deformation is then sent back to the fluid solver as a response of the given force. This process of transferring and receiving information, namely force and displacement, is then continued in an iterative loop until a certain convergence criteria is satisfied. In particular, the convergence criteria must preserve the continuity of velocity and position (or the Dirichlet conditions) as well as the equilibrium of forces (the Neumann condition) at the interface between the structure and the fluid domain. Ideally, one can write,

$$\begin{aligned} \boldsymbol{x}_{s\Gamma} &= \boldsymbol{x}_{f\Gamma}\,, \\ \boldsymbol{v}_{s\Gamma} &= \boldsymbol{v}_{f\Gamma}\,, \\ \boldsymbol{t}_{s\Gamma} &= \boldsymbol{t}_{f\Gamma}\,. \end{aligned} \tag{30}$$

where, $\boldsymbol{x}_\Gamma$, $\boldsymbol{v}_\Gamma$, and $\boldsymbol{t}_\Gamma$ are the position, velocity, and the traction vectors at the boundary, respectively, and the subscripts $s$ and $f$ indicate the partitioned structure and fluid parts. Therefore, the coupling loop between the structure and the fluid parts will always continue until convergence, up to certain given tolerance, of displacements $\boldsymbol{u}$ and forces $\boldsymbol{F}$ is reached, or until the maximum number of iteration is reached. In order to reach convergence, the Arbitrary Lagrangian Eulerian (ALE) scheme is also used to move the internal fluid mesh in such a way that it will always follow the structural displacements.

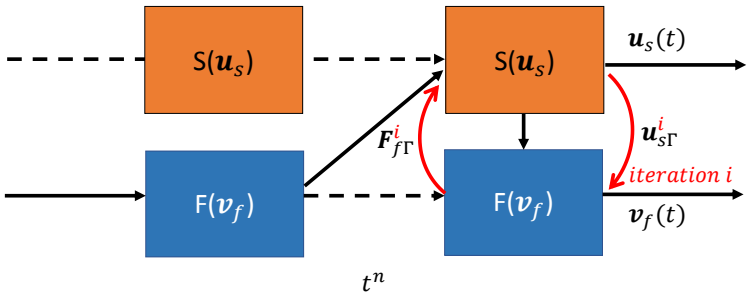


Figure 4: Solution algorithm for two-way coupling at every time step

# 3 Results and Analysis

This chapter describes the setup of the presented study including the specification of numerical parameters assumed. For the empirical study, most of the equations and assumptions are taken from [2], while for the CFD and FSI analysis, we ran the simulations it under the OpenFoam and Kratos Multiphysics framework. For the 1D MDOF structural solver, the simulation is implemented in a simple python code.

## 3.1 Empirical Study from the ASCE Design Code

A preliminary wind loading calculation using spread sheet is performed for a height interval of 5m. This calculation is done by considering a uniform velocity profile of the air on the width direction against the building. Using equation (6) we can plot the following gust velocity profile:

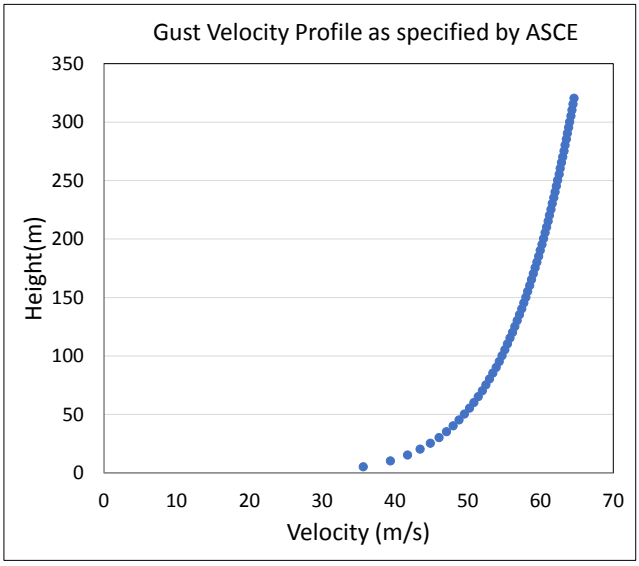


Figure 5: Velocity profile over height as calculated using ASCE design code

Furthermore, the design wind pressure calculation can be done by:

$$p(z) = q_z(z)G_f C_p - q_i G_{Cpi} \tag{31}$$

Here, $q_z(z)$ is the velocity pressure at each height calculated by equation (3), while $G_f$ and $C_p$ are the assumed gust effect factor and the external pressure coefficient, respectively. The constant parameters $q_i$

and $G_{Cpi}$ are nothing but the velocity pressure at the roof height of the building and the internal pressure coefficient. Here we assumed the following values specific for our problem type: $G_f = 0.99$, $C_p = 0.8$, and $G_{Cpi} = -0.18$, which are described in imperial units.

Furthermore, one can compute the wind load at varying height as:

$$F(z) = q_z(z) G_f C_f A_f \tag{32}$$

or, simpler,

$$F(z) = p(z) A_f(z) \tag{33}$$

Note that before calculating the force, we can convert the unit of the pressure value from imperial unit to SI unit.

Finally, the total approximated force and moment can be simply calculated by summing up all the force exerted on to the structure as:

$$F = \sum_{i=0}^{n_z} F_i \tag{34}$$

$$M = \sum_{i=0}^{n_z} F_i z_i \tag{35}$$

Notice here is that $n_z$ here is not the number of floor but the number of assumed height discretization. So for our case, since the height of the Empire State Building is about 380m and the height interval is $\Delta z = 5m$, we have $n_z = 76$. Using these equation, we obtained the total wind load and moment exerted to the building as $F = 27.24 \times 10^6$N and $M = 45.73 \times 10^8$Nm. We will validate these obtained values with the following CFD and FSI simulation to check its plausibility.

## 3.2 MDOF Structural Analysis

As what has been described in details at chapter 2, a one dimensional MDOF structural analysis is conducted in python considering the material parameters specified at table 1. In this model, we divided the whole structure into 102 degrees of freedom, which we obtained from the total number of floor at the Empire State Building. Here, we considered the time step $\Delta t = 10^{-3}$ and $\rho_\infty = 0.15$ for the generalized-$\alpha$ time integration. The following figure presents the first three natural modes of the building considering no damping.

These values can be compared with the Eurocode [4], which gives a rough estimation of the eigen-frequency for tall and slender buildings that is equal to $46/h$, where $h$ is the height of the building. In this case, the estimation of the first eigen-frequency by Eurocode yields to $\approx 0.12$Hz, which is reasonably close to our first eigen-frequency value.

We also checked the response displacement of our structural model with respect to the static wind load given by ASCE, which was calculated before at section 3.1. Here, we can say that our result of analysis lies within the safety criteria as written in the ASCE design code [2] and the serviceability limit states under wind load [9]. The obtained deformation is $\approx 1/19000$ fraction of the building height which, as stated in [9], is categorized as non-visible deformation with common damage of extremely minor cracking of brickwork.

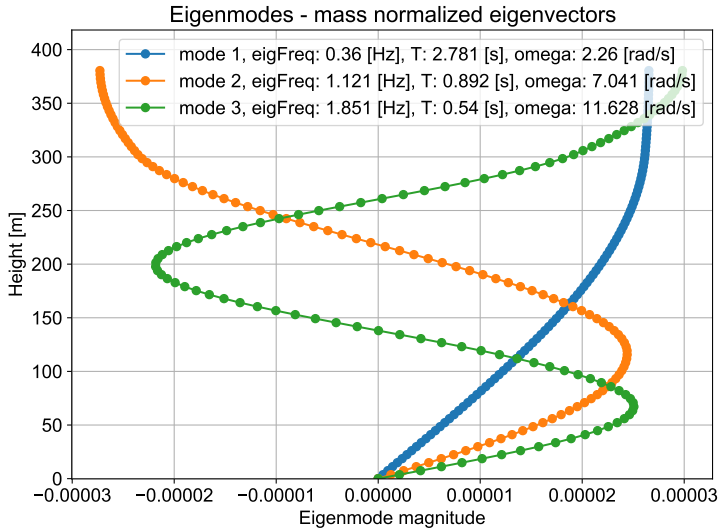


Figure 6: Natural modes of vibration, eigen-frequencies and periods of the building

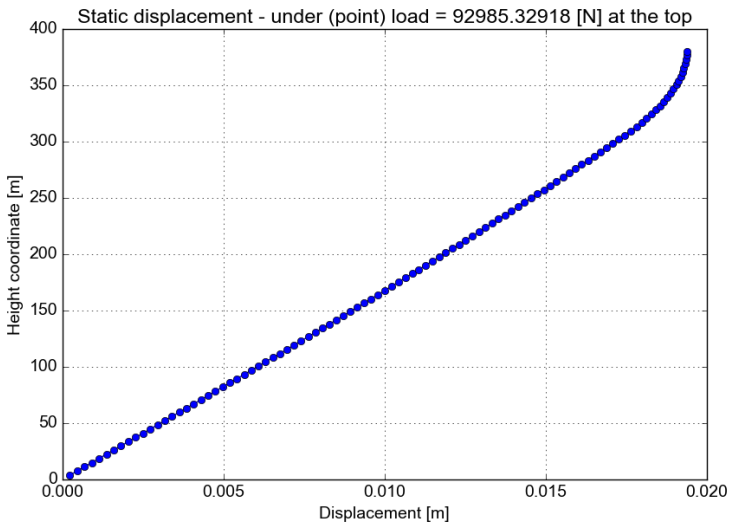


Figure 7: Response structural displacement due to static wind load by ASCE

## 3.3 3D CFD simulation in OpenFoam

### 3.3.1 System Setup

For computing a wind flow around a bluff body or an object, it is required to include a proper clearances of distance from the boundaries of the fluid domain. In general computational wind engineering simulation, it is necessary to satisfy less than 5% of admissible obstruction in the whole domain. However, since computing with the aforementioned criteria is computationally expensive, we decrease the size of our wind channel to a more appropriate size assuring that there are enough distances from the building towards the boundaries. In the current project, the computational domain for our wind flow simulation is set to be $W \times L \times H = 600[\text{m}] \times 1800[\text{m}] \times 600[\text{m}]$, which was chosen considering our building height $h = 380\text{m}$. We ran the CFD simulation for approximately 200s with $\Delta t = 0.03$.

Moreover, the material properties of our wind model is assumed to be Newtonian fluid with kinematic viscosity $\nu = 1.5 \times 10^{-5}[\mathrm{m}^2/\mathrm{s}]$. The fluid simulation is then run with the following boundary conditions:

- inlet: atmospheric boundary layer (ABL), zero gradient pressure
- outlet: total pressure of uniform zero value
- sides: slip
- ground: no-slip
- building: no-slip
- top: slip

The inlet wind velocity in our simulation is determined via the atmospheric boundary layer (ABL) class available in OpenFoam. This inlet class provides functions to evaluate the velocity and turbulence distributions appropriate for ABL of the specific surface roughness according to the terrain characteristic. Here, the profile is derived from the friction velocity, flow direction and "vertical" direction and written as:

$$U_{ABL} = \frac{U^*}{\kappa} \ln\left(\frac{z + z_0}{z_0}\right) \tag{36}$$

where, the friction velocity and the surface roughness is determined as $U^* = 3.462[\mathrm{m/s}]$ and $z_0 = 0.15[\mathrm{m}]$ with the assumption and calculations specified in [2]. Here, $\kappa = 0.41$ is the von Karman's constant. The following figure shows the modeled inlet condition using ABL in OpenFoam.

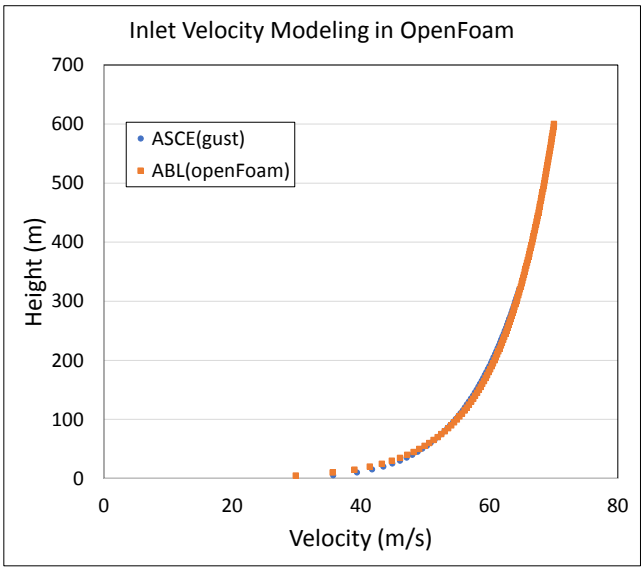


Figure 8: Inlet condition modeled by ABL

As it can be seen from the figure above, we can model the inlet velocity profile quite accurately compared to the computed gust velocity from the ASCE design code by equation (6).

### 3.3.2 Meshing

In a nutshell, SnappyHexMesh is a mesh generator that takes an already existing mesh (usually created with blockMesh) and chisels it into the desired mesh. From a triangulated surface geometry in Stereolithograpy

(STL) format, SnappyHexmesh automatically generates 3-dimensional meshes containing hexahedra and split-hexahedra. To generate a mesh with this mesh generator, the process starts with the generation of background mesh in the CFD domain. Using the OpenFOAM tool blockmesh, a basic mesh in the form of a rectangular box covering the entire simulation domain is created. This tool creates structured hexahedral elements at the depth of level 0. Following the preparing steps, snappyHexMesh continues with space-trees to refine the mesh around triangulated surfaces. The dictionary contains parameters for the three steps, castellatedMesh, snap, and addLayers, in three correspondent sub-dictionaries. These processes are done in an iterative manner and each step points to the specific level depth. The following step is the cell removal. Here, the cells, in the enclosed region by the STL surface, are removed. Moreover, cell splitting process or refinement can be conducted after this step by the user-defined bounding box. After refinement, boundary cells may now be adapted to the geometry. Last but not least, cell vertex points are moved onto the surface geometry to remove the jagged castellated surfaces from the mesh.

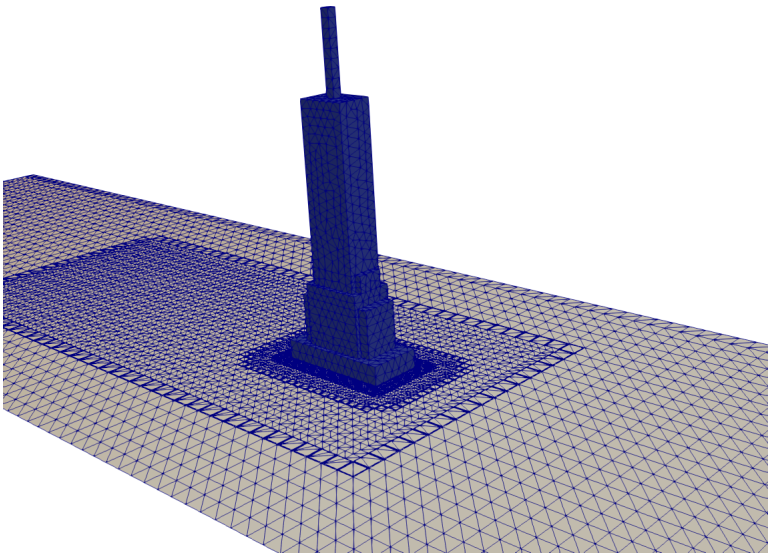

Figure 9: 3D meshing by SnappyHexMesh around the Empire State Building model

In the current project, we ran our CFD simulation in a total $\approx 3 \times 10^5$ cells, which are divided into three sub-domains separated by a defined bounding box. This bounding box is specified at the region where vortex shedding is expected behind the building, and thus, needs a finer mesh to resolve the turbulence flow characteristics. Outside this bounding box, the mesh is defined to be structural coarse grids, while inside the box, a finer one is expected. Moreover, nearby the building boundary, the SnappyHexMesh generates unstructured and surface fitted mesh with the finest resolutions. By doing this, we believe that we can obtain a more accurate wind pressure or loading exerted on the building.

#### 3.3.3 Analysis Results Considering Turbulence Models

In the following, the simulation results of our CFD wind simulation around the Empire State Building model are presented. The previously discussed turbulence models - the RANS k-$\epsilon$ model and the LES k-equation model are used to obtain the exerted wind loads in the rigid structure. The simulation results are presented and compared by Figure 10 and 11 in both top as well as the side cutting plane.

As what can be clearly seen from the analysis results, the vortex shedding is clearly formed as the wind flow pass the building. Here, the LES model is superior compared to the RANS model in order to preserve

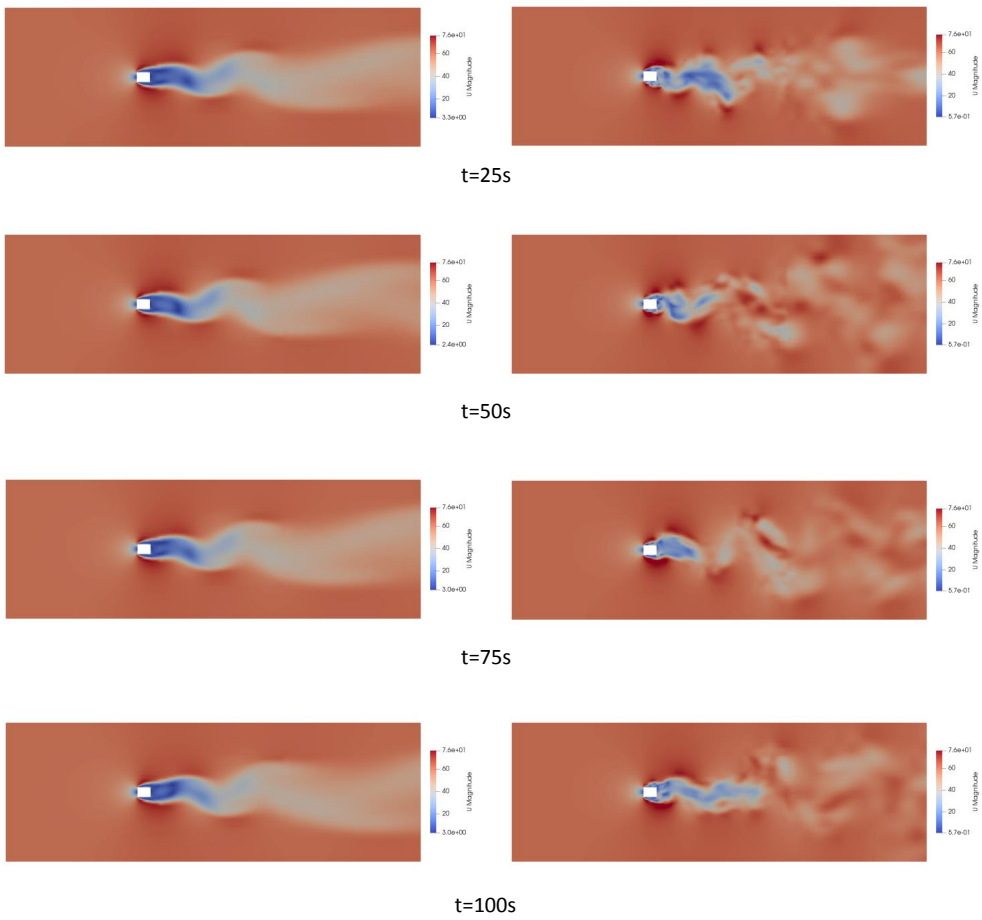


Figure 10: Comparison of vortex generated between the RANS k-$\epsilon$ model (left) and the LES k-equation model (right) at $h = 150m$ cutting plane.

much smaller eddies where the vortex are formed. However, as predicted, similar velocity profile can be captured by RANS and LES at different snapshot time of the simulation. Indeed, the RANS model has less capability in producing accurate velocity profile at particular region of the flow and especially when the time dependent solution is required. However, we found out that the RANS k-$\epsilon$ model is comparatively simpler to implement and leads to stable calculations that converge relatively easily. Meanwhile, the LES k-equation model is less stable, particularly at the beginning of the simulation, when the given wind velocity field is not presence at the whole domain. In the current project, the RANS model is run for the first ten seconds of the simulation, and then the LES model is started continuing the RANS velocity profile to overcome the aforementioned stability problem.

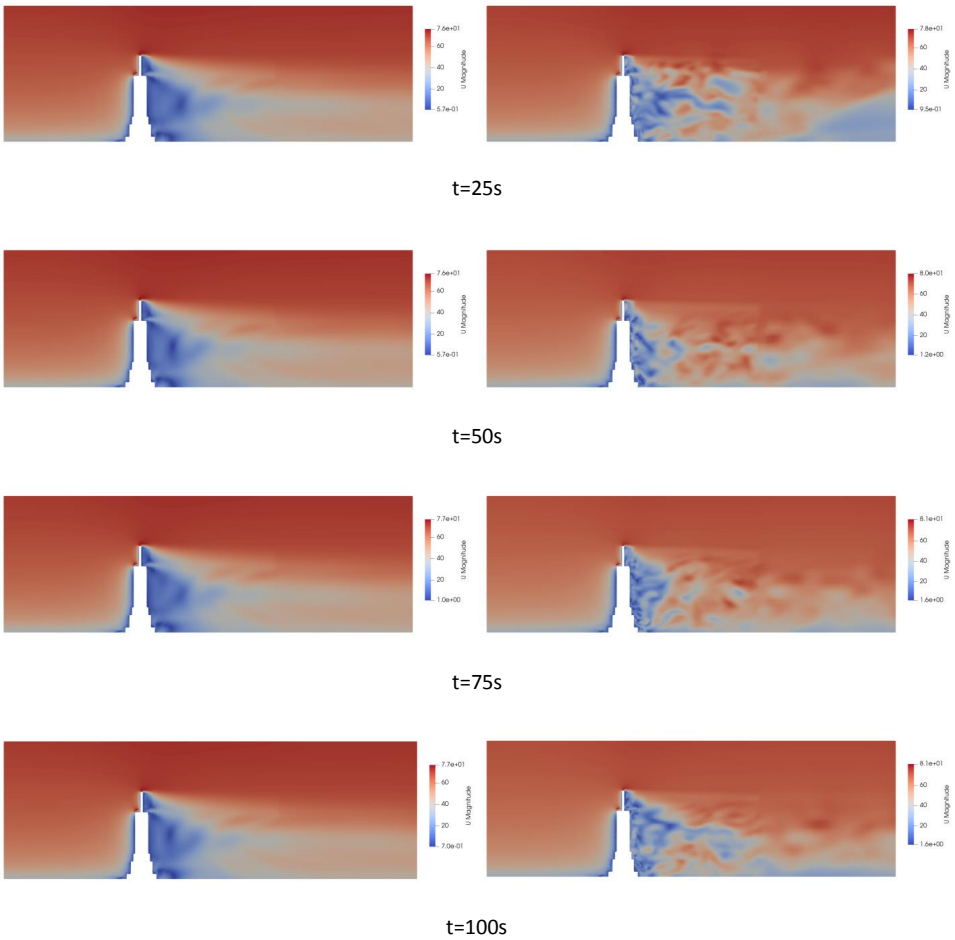


Figure 11: Comparison of CFD simulations between the RANS k-$\epsilon$ model (left) and the LES k-equation model (right) at half-side cutting plane.

The real motivation of this CFD simulation is to predict the dynamic wind load and moment exerted onto the building by the wind flow. The following figure 12 and 13 plot the comparison of the total wind forces and moment for the RANS and LES models. The total force here are obtained by integrating the pressure value obtained at the boundary with respect to area and the force caused by the viscosity, which is also significantly large for large side area like the Empire State Building. The moment is then calculated by multiplying the obtained force at each nodes with the node height $z_i$. Here, we can observe that the values calculated by the RANS model is slightly less than the one calculated by the LES model. A large different is also observed at the force and moment in the y-direction, which is predicted caused by the incapability of RANS model to accurately simulate flow around separation which create a lot of vortex shedding, and thus, results in forces in lateral direction.

From the obtained forces and moment in RANS and LES, we can obtained the average value of force magnitude $\bar{F}_{RANS} = 28.19 \times 10^6$N and $\bar{F}_{LES} = 30.71 \times 10^6$N. These values are very close to the obtained value calculated in section 3.1, which is $F = 27.24 \times 10^6$N. Moreover, the average value of moment magnitude $\bar{M}_{RANS} = 46.55 \times 10^8$Nm and $\bar{M}_{LES} = 50.48 \times 10^8$Nm, which are also significantly close to the pre-calculated moment $M = 45.73 \times 10^8$Nm.

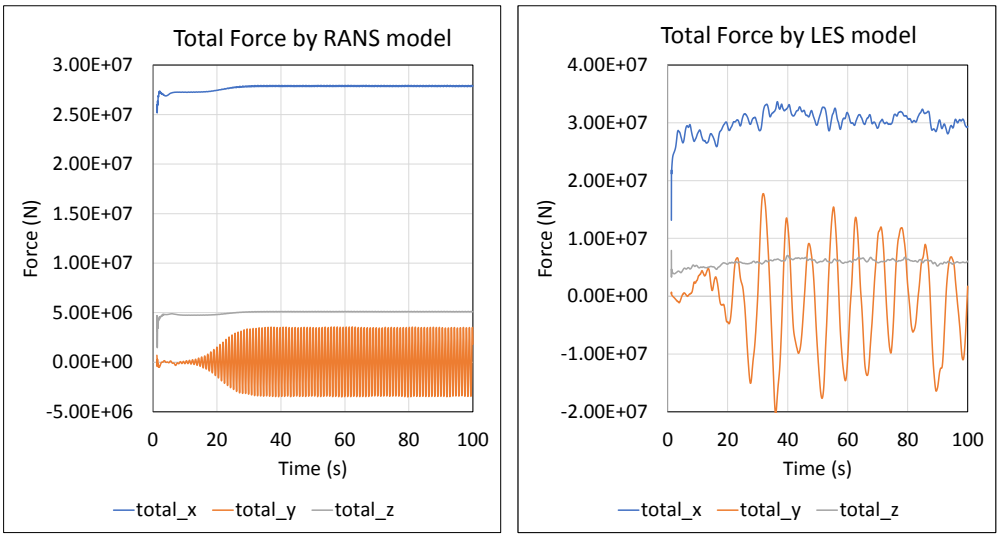


Figure 12: Comparison of total wind forces between the RANS k-$\epsilon$ model (left) and the LES k-equation model (right).

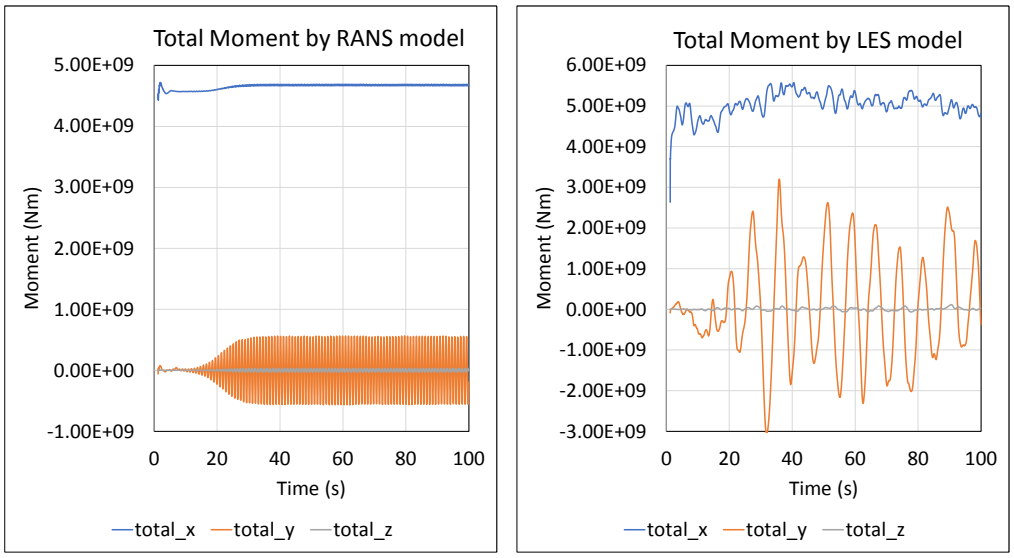


Figure 13: Comparison of total wind moment between the RANS k-$\epsilon$ model (left) and the LES k-equation model (right).

## 3.4 2D FSI simulation in Kratos Multiphysics

This chapter describes the setup of the 2D FSI simulation cases including the specification of numerical parameters. Here, we implemented a 2D MDOF solver for two different directions; lateral and longitudinal directions with respect to the wind inlet.

### 3.4.1 System Setup

Preprocessing the two-dimensional case requires the definition of the geometries and the assignment of corresponding boundary conditions. The length of the 2D wind channel 2400m, which is slightly larger to the one we had in 3D CFD, and the building is positioned at one forth of this length. The width of the

channel is 1200m and the building has a rectangular cross section of 56.7m×40.9m. The dimension of this cross section was chosen at the area of interest at height $150 \sim 180$m. Based on the described geometry, a mesh has to be generated and locally refined in the critical regions around the building. The triangles around the buildings have a side-length of 3m, the minimum throughout the entire mesh, whereas further cells are up to 10 times as large. In total, the mesh consists out of roughly 7600 triangle elements.

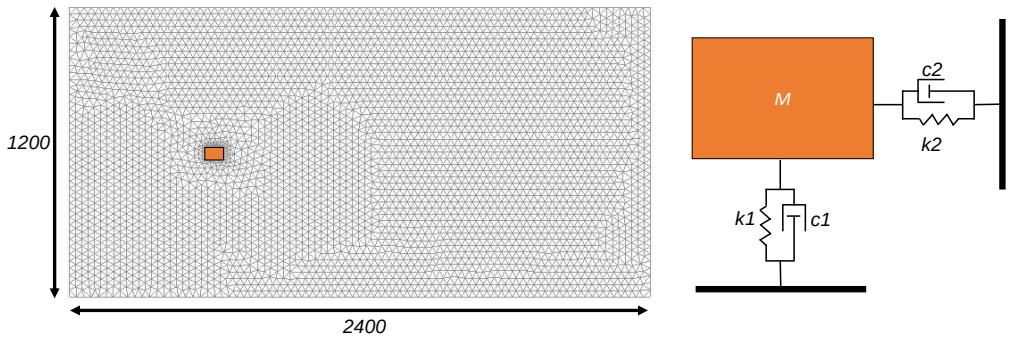


Figure 14: System setup for the 2D FSI with 2DOF structural model

The fluid enters the domain through the inlet boundary on the left edge. A constant velocity profile $v = 58.01$m/s was chosen referring to the obtained inlet velocity calculated by ASCE or ABL function. The side walls of the channel are defined as slip boundaries. In contrast, the building is assigned as a no-slip boundary condition and wall shear stresses can appear at their surface. Finally, the outlet on the right has a zero pressure boundary condition. The initial velocity field is constant 0m/s in the entire fluid domain. The inlet velocity profile is given a ramp-up time of 3s. Also the structures are set at rest at the beginning of the simulation.

The fluid is given approximately the physical properties of air, which is modeled as a Newtonian fluid with density $\rho = 1.2\text{kg/m}^3$ and kinematic viscosity $\nu = 1.5 \times 10^{-5}\text{m}^2/\text{s}$. The building is composed out of discrete elements, i.e. masses, dampers, and springs, as illustrated in Figure 14. Here, we only define the system as one block of mass with two DOFs in lateral and longitudinal wind directions. Notice that these two DOFs are independent of each other and uncoupled. We also do not consider the rotation angle as one of the DOFs, and thus, the building is assumed to be irrotational within its own axis. For our specific undamped case, we assumed that the mass $M = 3,656.9$ton, $k_1 = k_2 = 3.24 \times 10^{14}$N/m, and $c_1 = c_2 = 0.0\text{Ns/m}^2$. These selections of parameters are calculated according to the uniform distribution and linear interpolation of the parameters specified in table 1.

### 3.4.2 Analysis Results

The following figures plot the recorded wind load exerted on to the structure as well as it's response displacement. The force and displacement value plotted in blue for the x direction explain the buffeting phenomena caused by the wind flow. Meanwhile, the plotted force and displacement value in red correspond to the vortex shedding happen at the lateral y-direction. By analyzing these results, we can obtain the frequency of vortex shedding approximately to be $\approx 0.1$Hz, which lies in the range of $0.1 \sim 0.15$Hz specified by [11]. This value is then compared with the structural eigen-frequency estimated at section 3.2 which is 0.36Hz. Here, we can deduce qualitatively that the building lies on the safe side as the computed vortex shedding frequency is less than the structural eigen-frequency. One important factor that we can obtain

from the FSI analysis is the displacement value of the building at the desired height. However, since all the other methods only consider rigid structure or one-dimensional static loading, we unfortunately cannot compare the obtained results.

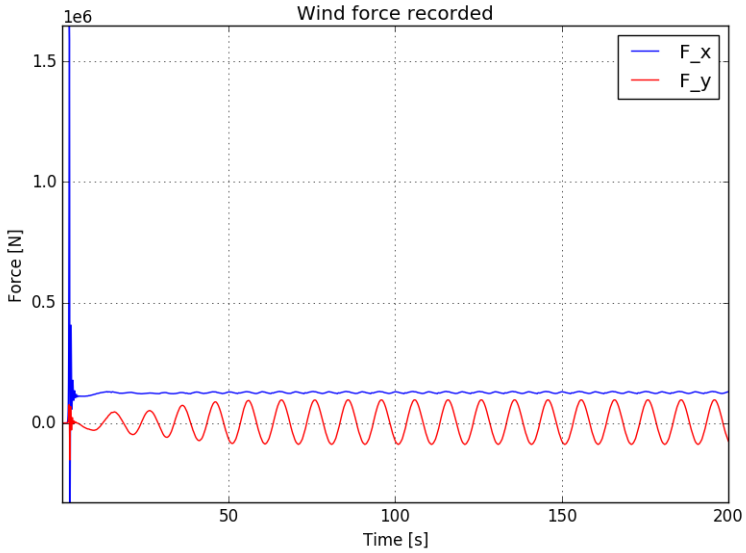


Figure 15: Wind loadings exerted on to the structure

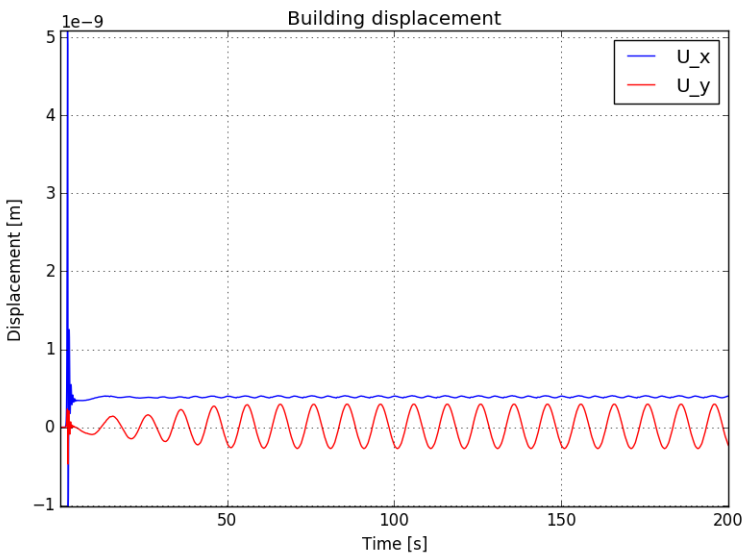


Figure 16: Building displacement with respect to the wind load

# 4 Conclusions

The impact of wind flow presents an important and significant effect, particularly on to the high-rise structures such as the Empire State Building. Using the available design codes and several open-source simulation tools such as OpenFoam and Kratos Multiphysics, structural wind analysis were performed in a simpler fashion to analyze the impact of wind flow onto the building model. Here, several types of analyses were performed to validate and check the plausibility of each methods. First, the analysis using the available design code is conducted. Here, we can obtained the wind force and moment for the

given wind model. Our results shown that these computed values are matching with the analysis results performed in the CFD and FSI analyses. For the CFD analysis, the total of 3.5% and 1.8% error can be observed in the time average force and moment predicted by RANS k-$\epsilon$ model in comparison with the value precalculated by the design code. Meanwhile, the LES k-equation model gives a slightly larger deviation of 12.7% and 10.4% difference for the estimated force and moment compared with the estimated design value. Even though that there are slight difference in these values, the values still lie at the same order of magnitude, which is considerably a remarkable result. Moreover, the simulation performed on the MDOF structural analysis also gives an adequate eigen-frequency in comparison with the vortex shedding frequency obtained at the FSI simulation. All and all, the conducted analyses give us a valuable understanding of several different approaches possible to analyze the impact of wind loading to a high-rise building.

# References


[1] A Bonelli et al.
"Analyses of the Generalized-$\alpha$ method for linear and non-linear forced excited systems".
In: *Structural Dynamics-EURODYN, vol. 2, pp. 1523-1528.*
2002.

[2] American Society of Civil Elilgineers.
*ASCE Standard: Minimum Design Loads for Buildings and Other Structures.*
American Society of Civil Engineers, 2002.

[3] Silvano Erlicher, Luca Bonaventura, and Oreste S Bursi.
"The analysis of the generalized-$\alpha$ method for non-linear dynamic problems".
In: *Computational Mechanics* 28.2 (2002), pp. 83–104.

[4] CEN Euroeode.
"4: design of composite steel and concrete structures. part 1-1: general rules and rules for buildings".
In: *German version ENV1994, O1-01* (1992).

[5] The OpenFOAM Foundation.
*OpenFOAM: k Equation.*
URL: `https://www.openfoam.com/documentation/cpp-guide/html/guide-turbulence-les-k-eqn.html`.

[6] The OpenFOAM Foundation.
*OpenFOAM: k-epsilon.*
URL: `https://www.openfoam.com/documentation/cpp-guide/html/guide-turbulence-ras-k-epsilon.html`.

[7] The OpenFOAM Foundation.
*OpenFOAM.*
URL: `https://openfoam.org/`.

[8] Wikipedia Foundation.
*Empire State Building - Wikipedia.*
URL: `https://en.wikipedia.org/wiki/Empire_State_Building`.

[9] Lawrence G Griffis.
"Serviceability limit states under wind load".
In: *Engineering journal/American institute of steel construction* (2003).

[10] F Moukalled, L Mangani, M Darwish, et al.
"The finite volume method in computational fluid dynamics".
In: (2016).

[11] Anna Agata Mueller.
*Large Eddy Simulation of cross-flow around a square rod at incidence with application to tonal noise prediction.*
University of Twente [Host], 2012.

[12] CM Rhie and WL Chow.
"Numerical study of the turbulent flow past an airfoil with trailing edge separation".
In: *AIAA Journal(ISSN 0001-1452)* 21 (1983), pp. 1525–1532.

[13] Yukio Tamura and Ryuichiro Yoshie.
*Advanced Environmental Wind Engineering.*
Springer, 2016.